Pion-Hyperon Resonances*

MARGARET H. ALSTON AND MASSIMILIANO FERRO-LUZZI†

Lawrence Radiation Laboratory, University of California, Berkeley, California

I. INTRODUCTION

RECENTLY a resonance in the $\Lambda-\pi$ system called Y_1^* has been observed, with a total energy of 1385 Mev.[1–6] This paper reviews and discusses the experimental data available as of February, 1961. Data from the first two experiments, which were performed at Berkeley using the 15-in. hydrogen bubble chamber, are discussed in some detail and the data combined wherever possible. Other data are used to show the effect of the resonance in various interactions.

II. THEORETICAL PREDICTIONS

Resonances in the pion-hyperon system have been predicted and are of two kinds: those arising from global symmetry and those resulting from bound states in the $\bar{K}-N$ system.

Global symmetry predicts two spin-$\frac{3}{2}$ pion-hyperon resonances,[7] one with isospin $T=1$, the other with $T=2$. These are the hyperon counterparts of the $J=T=\frac{3}{2}$ resonance of the pion-nucleon system. No counterpart can appear in the $J=\frac{3}{2}$, $T=0$ or in the $J=\frac{1}{2}$ states. The relevant kinematical data for the $\pi-N$ resonance and the $\pi-Y$ system with $T=1(Y_1^*)$ are shown in Table I. The $T=1$ resonance is predicted with a total energy of about 1375 Mev and a half-width $\Gamma/2=22$ Mev.[8] The value of the half-width is derived from the observed 45-Mev half-width of the pion-nucleon resonance after correcting for the difference in the c.m. momenta for the two cases $[(P_\Lambda/P_p)^3=0.73]$ and taking into account the restrictions on the decay rate[9] due to decay into the $\Sigma-\pi$ mode $[\frac{2}{3}]$. The Y^* with $T=1$ can decay into either a $\Lambda-\pi$ or $\Sigma-\pi$ system, the predicted Σ/Λ branching ratio R being about 5% for each charge state of the Σ.[9] The $T=2$ resonance is expected to have a larger mass value of about 1530 Mev, and a half-width of about 60 Mev.[8] These predictions depend upon the values of the pion-hyperon coupling constants used, and are obtained by assuming that $f_{\pi N}^2=f_{\pi\Sigma}^2=f_{\pi\Lambda}^2$.

In the $\bar{K}-N$ *"bound-state"* model,[10] $\Lambda-\pi$ and $\Sigma-\pi$ resonances arise from the $\bar{K}$ interactions and are a consequence of the properties of s-wave $\bar{K}-N$ scattering. The zero-energy K^-+p data permit a fourfold ambiguity in the solution for the scattering length; only two of the solutions (the "minus" ones) give $Y-\pi$ resonances since, to obtain a resonance below the $\bar{K}-N$ threshold, the real part of the scattering amplitude must be negative. The a_- solution[11] predicts a $T=1$ resonance in both the $\Lambda-\pi$ and $\Sigma-\pi$ systems at a total energy of 1382 ± 20 Mev with a half-width $\Gamma/2$ of 18 Mev and a possible $T=0$ resonance at a lower energy. The b_- solution[12] predicts a $T=0$ resonance with a total energy near 1420 Mev and possibly a $T=1$ resonance at lower energy. In both cases, the s-wave $\bar{K}-N$ bound state has total angular momentum $J=\frac{1}{2}$ and breaks up into $\Lambda+\pi$ via $S_{\frac{1}{2}}$ wave if the $K-Y$ parity is odd and $P_{\frac{1}{2}}$ if the $K-Y$ parity is even. This model predicts a value of the Σ/Λ branching ratio R of 15–80%,[11] the magnitude depending upon the assumptions made and in particular upon the relative $\Lambda-\Sigma$ parity.

TABLE I. Kinematical data for the pion-nucleon $J=\frac{3}{2}$, $T=\frac{3}{2}$ resonance and the pion-hyperon $J=\frac{3}{2}$, $T=1$ resonance.

Strong decay	Q (Mev)	P_π, c.m. (Mev/c)		$\Gamma/2$ (Mev)
$N_{\frac{3}{2}}^*\Rightarrow N+\pi$	159	230	$\left(\frac{P_\Lambda}{P_N}\right)^3=0.73$	45[a]
$Y_1^*\Rightarrow\Lambda+\pi$	130	207	$\left(\frac{P_\Sigma}{P_\Lambda}\right)^3=0.23$	23[b]
$Y_1^*\Rightarrow\Sigma+\pi$	50	127		

[a] Experimental value.
[b] Predicted value.

The experimental data are at present insufficient to distinguish between the two possible interpretations of the observed resonance, since interference effects (see Sec. III.F) make the determination of the spin and parity inconclusive.

* Work done under the auspices of the U. S. Atomic Energy Commission.

† National Academy of Sciences Fellow.

[1] M. Alston, L. W. Alvarez, P. Eberhard, M. L. Good, W. Graziano, H. K. Ticho, and S. G. Wojcicki, Phys. Rev. Letters **5**, 520 (1960).

[2] J. P. Berge, P. Bastien, O. Dahl, M. Ferro-Luzzi, J. Kirz, D. H. Miller, J. J. Murray, A. H. Rosenfeld, R. D. Tripp, and M. B. Watson, Phys. Rev. Letters **6**, 557 (1961).

[3] O. Dahl, N. Horwitz, D. H. Miller, J. J. Murray, and P. G. White, Phys. Rev. Letters **6**, 142 (1961).

[4] R. K. Adair, Revs. Modern Phys. **33**, 406 (1961), preceding paper.

[5] M. M. Block (private communication).

[6] R. P. Ely, S. Y. Fung, G. Gidal, Y. L. Pan, W. M. Powell, and H. White (private communication).

[7] M. Gell-Mann, Phys. Rev. **106**, 1296 (1957).

[8] D. Amati, B. Vitale, and A. Stanghellini, Phys. Rev. Letters **5**, 524 (1960).

[9] If we assume global symmetry, the branching ratios are

$$Y_1^{*\pm}\Rightarrow\Lambda+\pi^\pm:\Sigma^\pm+\pi^0:\Sigma^0+\pi^\pm=4:1:1$$

and

$$Y_1^{*0}\Rightarrow\Lambda+\pi^0:\Sigma^0+\pi^0:\Sigma^+\pi^-:\Sigma^-+\pi^+=4:0:1:1.$$

The relative Σ ratios are independent of global-symmetry arguments and follow from charge independence only. The Σ/Λ branching ratios then have to be corrected by the appropriate phase-space factor $[(P_\Sigma/P_\Lambda)^3=0.23$, see Table I$]$.

[10] R. H. Dalitz and S. F. Tuan, Phys. Rev. Letters **2**, 425 (1959); Ann. Phys. **8**, 100 (1959); **10**, 307 (1960).

[11] R. H. Dalitz, Phys. Rev. Letters **6**, 239 (1961).

[12] R. L. Schult and R. H. Capps (private communication).

TABLE II. Distribution of events and cross sections (in parentheses) among different reactions for different values of the incident K^- momentum. P_K cross sections in mb.

Reaction	K^- momentum (Mev/c) 510	620	760	850	1150
$K^-+p\rightarrow\Lambda+\pi^++\pi^-$	30	54	262	153	49
$(\Lambda$ or $\Sigma^0)+\pi^++\pi^-$	2 (1.5±0.3)	2 (2.1±0.3)	41 (3.6±0.3)	37 (3.5±0.3)	92 (4.1±0.4)
$\Sigma^0+\pi^++\pi^-$	9	10	51	35	27
$(\Lambda$ or $\Sigma^0)+\pi^++\pi^-+\pi^0$	0 (0)	0 (0)	20 (0.20±0.05)	7 (0.11±0.04)	39 (1.1±0.2)
$\bar{K}^0+p+\pi^-$	0 (0)	0 (0)	2 (0.03±0.02)	3 (0.03±0.02)	48 (2.0±0.3)
Total events	41	66	376	235	255

III. PRODUCTION OF Y^* IN THE REACTION $K^-+p\rightarrow Y^*+\pi$

A. General

The $\Lambda-\pi$ resonance has been observed in experiments performed at Berkeley using the 15-in. hydrogen-filled bubble chamber and separated K^- beams.[13,14] The first experiment was at 1.15 Bev/c incident K^- momentum.[1] Currently a study[2] of the process for incident K^- momenta from 850 Mev/c down to the $\Lambda-\pi$ resonance threshold of 405 Mev/c is being made. In these experiments, Y^* should be observed in the reactions

$$K^-+p\rightarrow\Lambda+\pi^++\pi^- \quad (1)$$

$$\Sigma^0+\pi^++\pi^- \quad (2)$$

$$\Sigma^-+\pi^++\pi^0 \quad (3)$$

$$\Sigma^++\pi^-+\pi^0. \quad (4)$$

A total of about 1000 interactions which appear in the bubble chamber as a two-prong event plus a V have been analyzed. Table II illustrates their apportioning between the various possible reactions. An event was placed in a definite category if the χ^2 probability for other hypotheses was $\leqslant 1\%$, or was considered ambiguous if both hypotheses (Λ or Σ^0) had a χ^2 probability $\geqslant 1\%$.

B. Dalitz Plots for Reaction (1)

A simple and suggestive way of illustrating the occurrence of the reaction $K^-+p\rightarrow Y_1^{*\pm}+\pi^{\mp}$ is Dalitz' representation,[15] which consists of displaying the events on a $T_{\pi^+}-T_{\pi^-}$ plane (T=kinetic energy in the reaction center of mass). In this plot, unit area is proportional to phase space so that the density of the events is proportional to the matrix element. Thus, if there is no coupling between any two particles in the final state, the points representing the events are

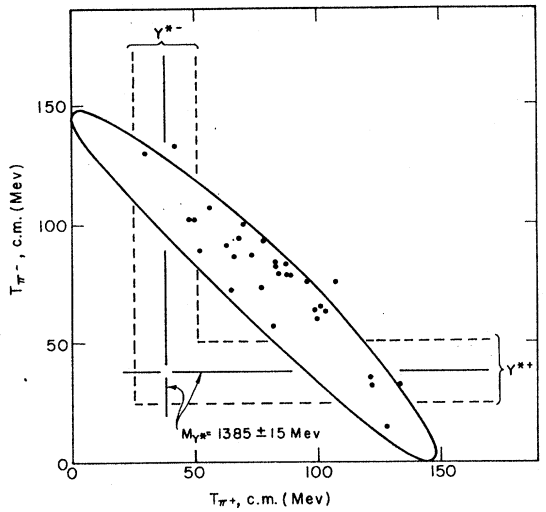

FIG. 1. Dalitz plot for the reaction $K^-+p\rightarrow\Lambda+\pi^++\pi^-$ at $P_{K^-}=510\pm20$ Mev/c (31 events).

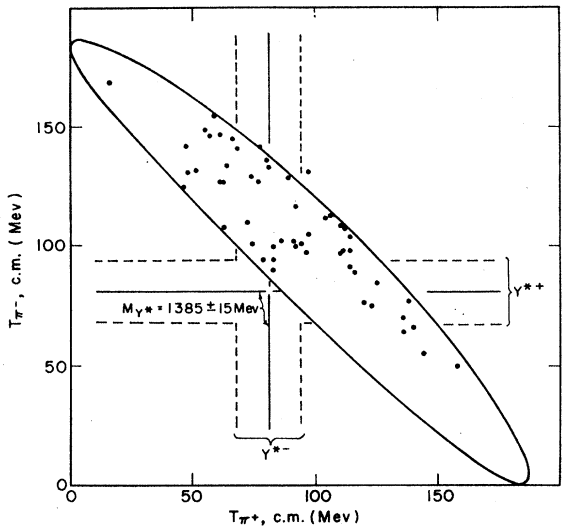

FIG. 2. Dalitz plot for the reaction $K^-+p\rightarrow\Lambda+\pi^++\pi^-$ at $P_{K^-}=620\pm15$ Mev/c (54 events).

[13] P. Eberhard, M. L. Good, and H. K. Ticho, Rev. Sci. Instr. 31, 1054 (1960).

[14] P. Schlein, P. Bastien, O. Dahl, J. J. Murray, M. Watson, R. G. Ammar, paper presented at the International Conference on Instrumentation for High-Energy Physics, Berkeley, 1960.

[15] M. Gell-Mann and A. H. Rosenfeld, Ann. Rev. Nuclear Sci. 7, 407 (1957), Appendix C.

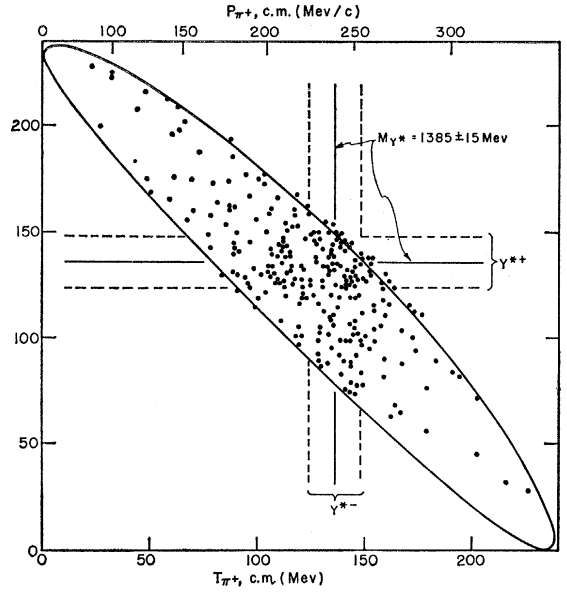

FIG. 3. Dalitz plot for the reaction $K^-+p\rightarrow\Lambda+\pi^++\pi^-$ at $P_{K^-}=760\pm7.5$ Mev/c (262 events).

expected to lie uniformly over the allowed kinematical region. In contrast to this three-body model, we can consider the two-body reaction in which a Y^*, of fixed mass and zero width, and a pion are produced. In this case, the events must lie on a horizontal or vertical line associated with a unique T_π. Actually, Y^* is a resonance of finite width (Γ) and does not lie on a line but is spread over a finite band of the Dalitz plot. The relation between pion kinetic energy and Y^* mass is simply

$$dM_{Y^*}/dT_\pi=-E/M_{Y^*}, \tag{5}$$

where E is the total energy in the c.m. system.

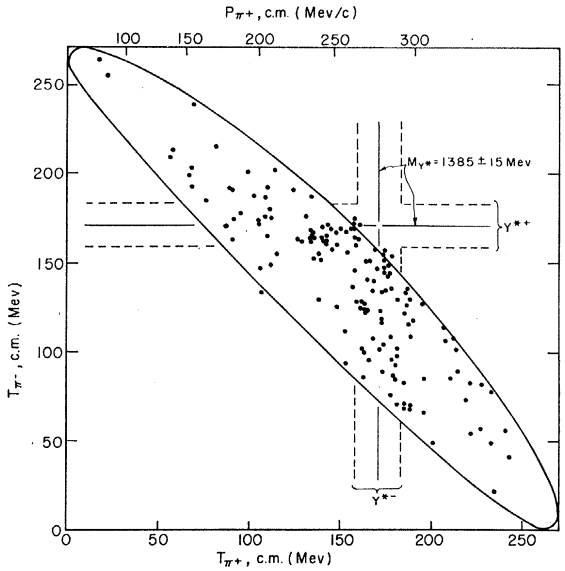

FIG. 4. Dalitz plot for the reaction $K^-+p\rightarrow\Lambda+\pi^++\pi^-$ at $P_{K^-}=850\pm10$ Mev/c (153 events).

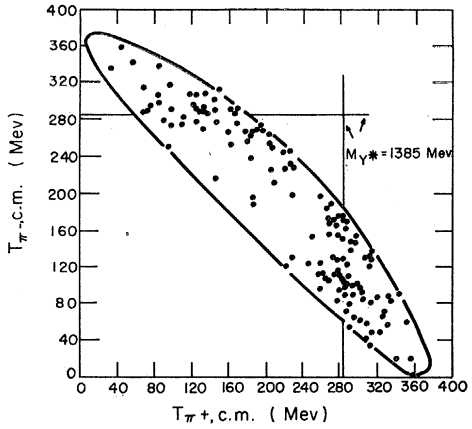

FIG. 5. Dalitz plot for the reaction $K^-+p\rightarrow\Lambda+\pi^++\pi^-$ at $P_{K^-}=1150\pm25$ Mev/c (141 events).

dM_{Y^*}/dT_π goes from -1.1 at $P_K=510$ Mev/c to -1.35 at $P_K=1150$ Mev/c.

Figures 1–5 show these Dalitz plots. All ambiguous (Λ or Σ^0) events were plotted in the 1.15-Bev/c diagram because estimates showed that most of these were Λ's. In the lower momenta plots, no ambiguous events were used. It may be seen that no evidence for pronounced crowding along the predicted lines occurs for the lower momenta while a definite correlation is noticeable at 760, 850, and 1150 Mev/c.

A more qualitative approach is obtained by projecting the points of the Dalitz plots onto either axis. In order to separate Y_1^{*+} from Y_1^{*-}, the convention has been adopted of splitting the kinematical area into two equal parts by a 45-deg line and assigning different signs to

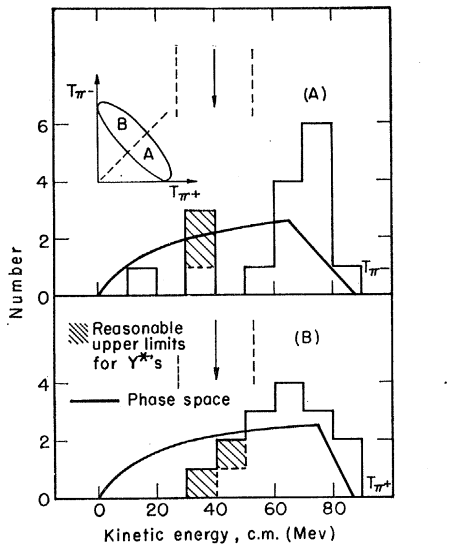

FIG. 6. Pion kinetic-energy spectra in c.m. for the reaction $K^-+p\rightarrow\Lambda+\pi^++\pi^-$ at $P_{K^-}=510\pm20$ Mev/c. Only negative (positive) pions belonging to events in the A (B) region of the corresponding Dalitz plot appear in the histograms. The phase-space curve indicates the amount of distortion introduced by this separation. The dotted lines correspond to $M_{Y^*}=1385\pm15$ Mev.

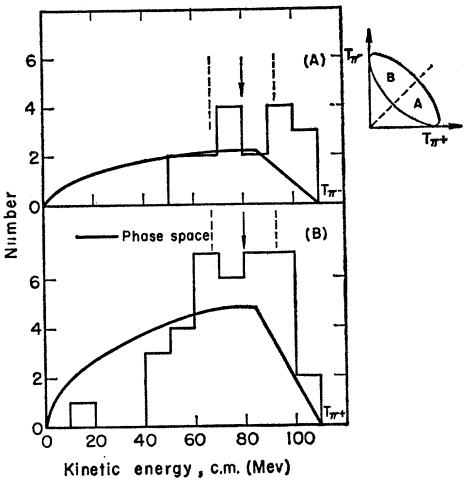

FIG. 7. Pion kinetic energy spectra in c.m. for the reaction $K^-+p\rightarrow\Lambda+\pi^++\pi^-$ at $P_{K^-}=620\pm15$ Mev/c. Only negative (positive) pions belonging to events in the A (B) region of the corresponding Dalitz plot appear in the histograms. The phase-space curve indicates the amount of distortion introduced by this separation. The dotted lines correspond to $M_{Y^*}=1385\pm15$ Mev.

the events on the two sides. These T_{π^+} and T_{π^-} histograms appear in Figs. 6–10, where also a phase-spaec curve has been drawn for comparison. We should comment on the difficulties introduced into these projections by this arbitrary division of the Dalitz plot.

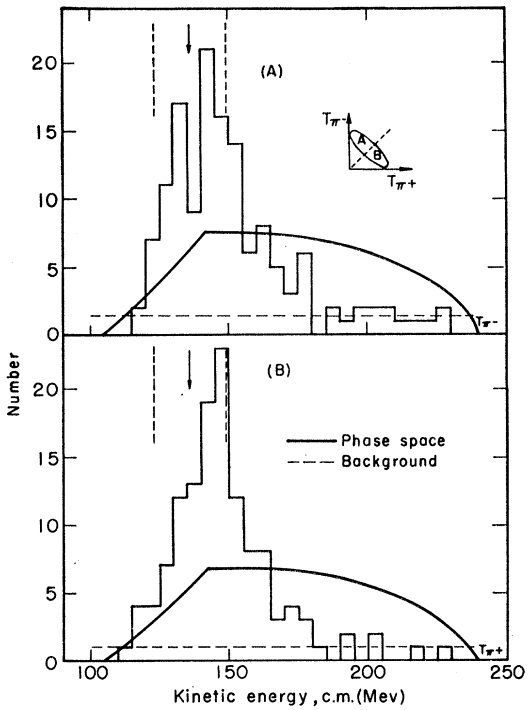

FIG. 8. Pion kinetic-energy spectra in c.m. for the reaction $K^-+p\rightarrow\Lambda+\pi^++\pi^-$ at $P_{K^-}=760\pm7.5$ Mev/c. Only negative (positive) pions belonging to events in the A (B) region of the corresponding Dalitz plot appear in the histograms. The phase-space curve indicates the amount of distortion introduced by this separation. The dotted lines correspond to $M_{Y^*}=1385\pm15$ Mev.

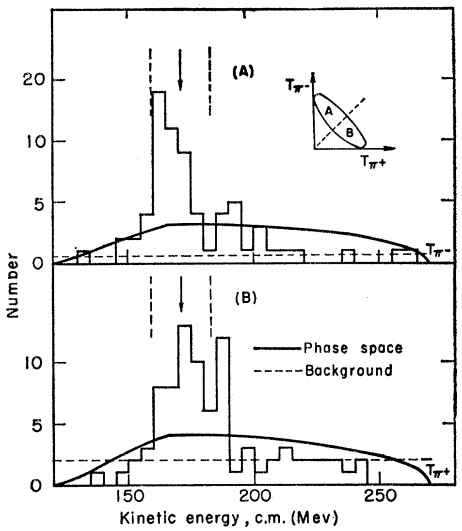

FIG. 9. Pion kinetic-energy spectra in c.m. for the reaction $K^-+p\rightarrow\Lambda+\pi^++\pi^-$ at $P_{K^-}=850\pm10$ Mev/c. Only negative (positive) pions belonging to events in the A (B) region of the corresponding Dalitz plot appear in the histograms. The phase-space curve indicates the amount of distortion introduced by this separation. The dotted lines correspond to $M_{Y^*}=1385\pm15$ Mev.

It can be seen that at 1150 Mev/c the bands are well separated. At 850 Mev/c they hardly overlap, the 45-deg line does not pass close to many events, and the projection is hardly influenced by the division. On the other hand, at the two lowest momenta, the shape of the resonance is completely mutilated by this procedure.

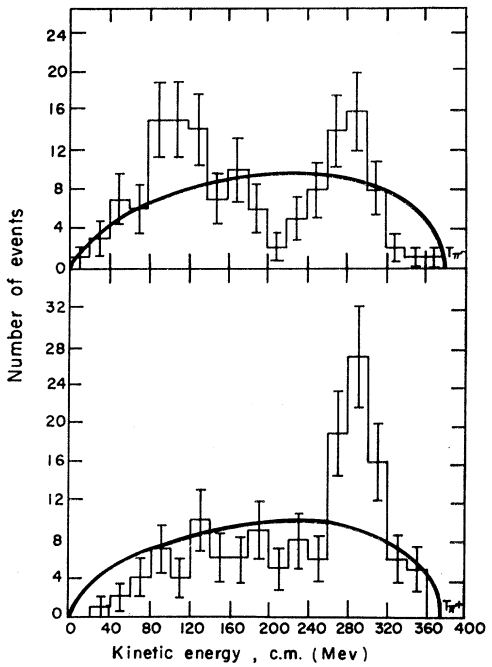

FIG. 10. Pion kinetic-energy spectra in c.m. for the reaction $K^-+p\rightarrow\Lambda+\pi^++\pi^-$ at $P_{K^-}=1150\pm25$ Mev/c. Here no division between Y^* charges has been made; curves drawn are undistorted phase space.

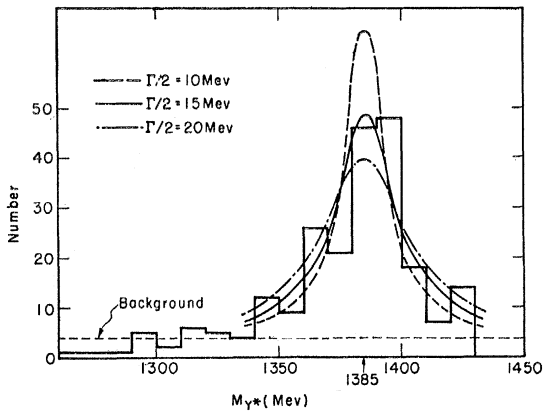

FIG. 11. Y^* mass spectrum from 226 $\Lambda\pi^+\pi^-$ events at $P_{K^-}=850$ Mev/c.

These mutilated projections are presented not because they contribute information on the shape of the resonance, but to illustrate the uncertainties in separating Y^* from background.

C. Mass and Width of Y_1^*

Inspection of Figs. 9 and 10 shows no appreciable $Y^{*+}-Y^{*-}$ mass difference. Hence, in Fig. 11 the combined $Y_1^{*+}+Y_1^{*-}$ mass spectrum is plotted for 850-Mev/c incident momentum. On this spectrum a background level is indicated and three normalized resonance curves of the form

$$\frac{dn}{dM}=\frac{\Gamma/2}{(M-1385)^2+(\Gamma/2)^2}\frac{N}{\pi} \tag{6}$$

are plotted (some small dependence on the decay momentum has been neglected). The best value of $\Gamma/2$ is about 15 Mev, and the choice of 1385 as a central value appears uncertain by $\lesssim\pm5$ Mev. A higher limit on the values of $\Gamma/2$ is about 20 Mev which is obtained when no background is subtracted from the spectrum.

Even this value of $\Gamma/2$ is smaller than that observed for the 1150 Mev/c spectrum (Fig. 12). Here no background has been subtracted and the fitted curve shows $\Gamma/2=32$ Mev. The uncertainty on the mass of each Y^* was computed from the fitted track variables and the variance-covariance matrix. For the 850-Mev/c events, this uncertainty is typically ±3 to ±5 Mev; for those at 1150 Mev/c, it is typically ±6 to ±10 Mev. There appears to be a definite discrepancy between $\Gamma/2$ as given by the 850- and 1150-Mev/c data. Adair has pointed out that there are reasons why the background may not be flat under the Y_1^* peaks[4]; the resonance curve at 1150 Mev/c could appear too wide just because it is superimposed on a broader maximum in the background. However, an even more convincing way of resolving this apparent disagreement results from the analysis of Dalitz and Miller (see Sec. III.F).

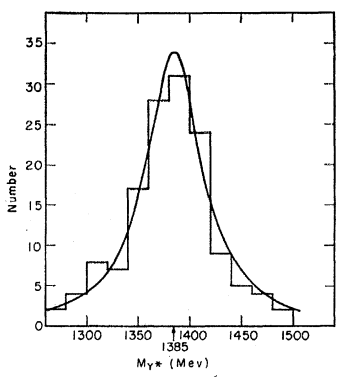

FIG. 12. Y^* mass spectrum from 141 $\Lambda\pi^+\pi^-$ events at $P_{K^-}=1150$ Mev/c. $\Gamma/2=32$ Mev.

D. Y_1^* Excitation Function

To obtain the total cross section and excitation functions for the reactions (1) and (2), we have estimated the number of ambiguous events that were probably Λ's. For all incident momenta less than 1150 Mev/c, the number of ambiguous events was quite small and they were assigned to definite categories in the ratio of the unambiguous events. However, in the 1150-Mev/c data, the number of ambiguous events is large. Estimates showed that, of the 92 ambiguous events, 13 were more probably Σ^0 than Λ. The total cross sections for all reactions are shown in Table III and the cross section for the $\Lambda\pi^+\pi^-$ final state plotted in Fig. 13, which also shows the estimated cross sections for Y_1^{*+} and Y_1^{*-} production.

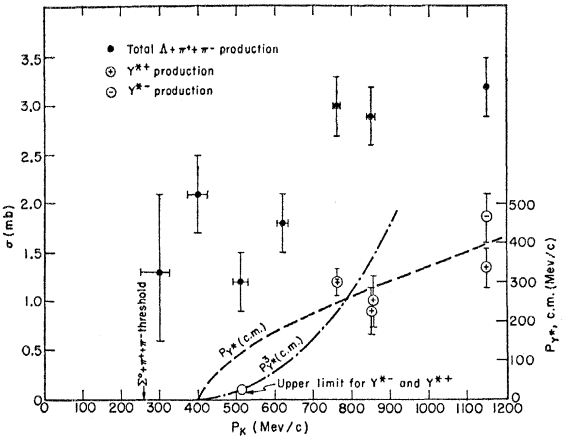

FIG. 13. Excitation data for the total $\Lambda\pi^+\pi^-$ production and its apportioning into Y^{*+} and Y^{*-}. The dashed curves are P_{Y^*}(c.m.) and $P_{Y^{*3}}$(c.m.) as a function of P_{K^-}(lab). Points at 300 and 400 Mev/c represent very preliminary values.

To obtain these cross sections, we have subtracted the three-particle final-state background. The cross section $\sigma(Y_1^*)$ at 850 Mev/c can be obtained fairly unambiguously from Fig. 9, which displays dashed lines assumed to be background. We define all excess over background as Y_1^*. For 760 Mev/c (Fig. 8), the foregoing prescription is still fairly satisfactory, but at 620 Mev/c it becomes meaningless. Inspection of Fig. 6

TABLE III. Number of events and cross sections (in parentheses) for Y^* production at different values of the incident K^- momentum. Cross sections in mb.

Reaction	K^- momentum (Mev/c) 510	620	760	850	1150
$\Lambda\pi^+\pi^-$ Y^{*-}	<2 (0.1)	56 (1.8±0.3)	121 (1.2±0.14)	56 (0.9±0.25)	75 (1.8±0.3)
$\Lambda\pi^+\pi^-$ Y^{*+}	<2 (0.1)		122 (1.2±0.14)	62 (1.0±0.25)	53 (1.3±0.2)
$\Lambda\pi^+\pi^-$ Three-body	>28 (1.0)		56 (0.6±0.1)	67 (1.0±0.15)	0

(510 Mev/c) shows that it is artificial to designate as Y_1^{*-} more than two events out of the 16 in the T_{π^+} projection. This gives an upper limit of 0.1 mb for $\sigma(Y_1^{*-})$ at 510 Mev/c. Although no value can be plotted at 620 Mev/c, we believe that it should be quite small because below the Y_1^* threshold (405 Mev/c) the $\Lambda\pi^+\pi^-$ "background" averages about 2 mb and we assume that σ (background) varies fairly smoothly. Also shown on Fig. 13 are the curves for s- and p-wave production of the Y_1^* assuming a two-body final state ($Y_1^*+\pi$). Despite the uselessness of the 620-Mev/c data, the apparently low $\sigma(Y_1^*)$ at 510 Mev/c does suggest that the Y_1^* excitation function is already dominated by p-wave production at 510 Mev/c.

Two reasons for p-wave dominance have been advanced: (1) Dalitz[11] has pointed out that it is natural for pions to be emitted in p waves by nucleons as, for example, in the reaction $p+p\rightarrow\pi^++d$. The same mechanism can apply, though perhaps not so strongly, to the reaction $K^-+N\rightarrow\pi+(\bar{K}N)^*\rightarrow\pi+Y^*$. (2) Sawyer[16] has remarked that if Y_1^* is the $P_{\frac{3}{2}}$ global symmetry resonance, then the KY^* parity is the same as the $K\Lambda$ parity (most likely odd). In this case, s-wave Y_1^* production can proceed only from a $D_{\frac{3}{2}}$ initial state. If $D_{\frac{3}{2}}$ is weakly absorbed, p-wave dominance in the final state is enhanced. Unfortunately, both explanations are reasonable, so the suggestion of a p-wave excitation function does not help to resolve the spin and parity of Y^*.

E. Y_1^* Production Angular Distributions and Polarization

If we assume a two-body final state, the production angular distribution can be written in the form $1+a\cos\theta_{KY^*}+b\cos^2\theta_{KY^*}+\cdots$, where θ_{KY^*} is the Y_1^* production angle. At 1150 Mev/c, there is a slight indication of some $\cos^2\theta_{KY^*}$ component for Y^{*+}. At the lower momenta, b may be considered equal to zero. The experimental values of a are shown in Table IV and indicate negligible deviations from isotropy except at the highest momentum.

The polarization P_{Y^*} of Y_1^* parallel to the normal $\hat{n}$ to the production plane can be measured by the chain of strong and weak decays: $Y_1^*\Rightarrow\Lambda+\pi$, $\Lambda\rightarrow p+\pi$. Any polarization P_Λ of the Λ indicates a polarization of the Y^*. The value of $\bar{P}_\Lambda$ can be calculated from the relation

$$\alpha\bar{P}_\Lambda=\frac{3}{N}\sum_{i=1}^{N}(\hat{n}\cdot\hat{p})\pm\left(\frac{3-(\alpha\bar{P}_\Lambda)^2}{N}\right)^{\frac{1}{2}}, \qquad (7)$$

where $\hat{p}$ is the unit vector along the proton momentum and α is the asymmetry coefficient in Λ decay ($\alpha\sim1$). Table IV summarizes $\alpha\bar{P}_\Lambda$ obtained from Eq. (7) using only events in which $|\cos\theta_{KY^*}|\leqslant0.85$. This selection was made because of the $\sin\theta_{KY^*}$ dependence of P_{Y^*}. The large value of $\alpha\bar{P}_\Lambda$ at 850 Mev/c confirms the evidence from the excitation function that Y_1^*'s (despite their isotropic production angular distribution at 760 and 850 Mev/c) cannot be assumed to be dominantly produced in s waves.

F. Interference Effects in Y_1^* Production

The oversimplified model in which Y_1^* is produced "isolated" in a two-body final state neglects the interference (a) between Y_1^* of opposite charge, (b) between Y_1^* and ($\Lambda\pi^+\pi^-$) produced in nonresonant background states, and (c) final-state interaction between π^+ and π^- and the influence of Bose statistics on this system.

A truly isolated Y_1^* cannot display any fore-aft asymmetry when it strong-decays. A way to measure the departure of the experimental situation from the "isolated" model is offered by the asymmetry coefficient

TABLE IV. Asymmetry coefficients and Λ polarization in Y^* production and decay for three incident momentum values.

Measured parameters (%)	K^- momentum (Mev/c) 760 Y^{*+}	760 Y^{*-}	850 Y^{*+}	850 Y^{*-}	1150 Y^{*+}	1150 Y^{*-}
Production a	+10±20	−4±20	+2±26	−10±24	−40±26	−30±20
Decay A	−24±20	−16±20	−92±26	−34±24	−70±26	−2±20
Λ polarization $\alpha\bar{P}_\Lambda$	−16±20	+10±20	+12±28	−56±20	+2±22	−30±20

[16] R. F. Sawyer (private communication by M. L. Good).

TABLE V. Number of events and cross sections (in parentheses) for Σ production at different values of the incident K^- momentum. Cross sections in mb.

Reaction	K^- momentum (Mev/c) 510	620	760	850	1150
$\Sigma^0\pi^+\pi^-$	9 (0.2±0.1)	10 (0.3±0.1)	55 (0.6±0.1)	39 (0.6±0.1)	40 (1.0±0.2)
$\Sigma^-\pi^+\pi^0$	a	a	a	a	55 (0.8±0.1)
$\Sigma^+\pi^-\pi^0$	a	a	a	a	57 (0.8±0.1)

[a] Not yet analyzed.

A in the Y_1^* strong-decay distribution:

$$1+A\cos\theta_{Y^*\Lambda}+B\cos^2\theta_{Y^*\Lambda}+\cdots, \quad (8)$$

where $\theta_{Y^*\Lambda}$ is the angle between the Y^* and the Λ in the Y^* c.m. system.

None of our data exhibit any evidence for $B\neq 0$, but $|A|$ is large (see Table IV) and shows that "isolation" is a poor approximation even at 1150 Mev/c. The sign of A is consistent with the fact that one expects $Y^{*\pm}$ to strong-decay with the Λ going backwards so as to favor resonance with the $\pi^{\mp}$.

Dalitz and Miller are currently making an analysis based on a three-body final state, taking into account the interference effects mentioned, with the exception of the $\pi-\pi$ interaction.[17] Preliminary results of this analysis give a satisfactory explanation of most of the experimental data. The difference in the observed width of the resonance at different incident momenta is automatically introduced by the interference mechanism, and the data at all incident momenta are found to be mutually consistent for a half-width of about 25 Mev. The distribution of events on the Dalitz plots allow only two interpretations: s-wave production of an $l=1$ Y_1^* or p-wave production of an $l=0$ Y_1^*. The asymmetry coefficients in the Y_1^* decay (Table IV) can also be explained by the model except those at 1150 Mev/c, where the effect is larger than that predicted.

G. Adair Analysis for the Spin of Y_1^*

If the model in which the Y_1^* is produced isolated were applicable, an Adair analysis would determine the Y_1^* spin.[18] A polar produced Y_1^* with $J>\frac{1}{2}$ is transversely aligned because there is no component of orbital angular momentum in the beam direction. The decay distribution of this Y_1^* is then uniquely determined by its spin. In particular, this distribution is of the form $1+3\cos^2\theta_{K\Lambda}$ for $J=\frac{3}{2}$, where $\theta_{K\Lambda}$ is the angle between the beam direction and the decay Λ in the Y^* c.m. For $J=\frac{1}{2}$, the Y_1^* is not aligned and its decay distribution is isotropic.

The experimental data combined for all incident momenta and all Y_1^*'s produced at $|\cos\theta_{KY^*}|\geqslant 0.90$ are shown in Fig. 14 together with the predicted distributions for $J=\frac{1}{2}$ and $\frac{3}{2}$. A χ^2 test gives 5:1 odds against $J=\frac{3}{2}$. This beautiful conclusion unfortunately seems to be completely irrelevant in view of the Dalitz-Miller arguments.[17] Their treatment gives very different Adair distributions from those predicted by the "isolated" model for both $J=\frac{1}{2}$ and $\frac{3}{2}$. In particular, at 850 Mev/c incident momentum, an s-wave $P_{\frac{3}{2}}$ Y_1^* and a p-wave $S_{\frac{1}{2}}$ Y_1^* yield two distributions which cannot be distinguished by the available data.

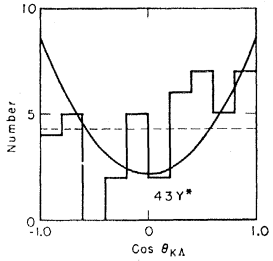

FIG. 14. Adair analysis for Y^* at $P_{K^-}=760$, 850 and 1150 Mev/c, and $|\cos\theta_{KY^*}|\geqslant 0.90$. - - - - $J=\frac{1}{2}$; —— $J=\frac{3}{2}$.

H. Branching Ratio

$$R=(Y_1^*\Rightarrow\Sigma+\pi)/(Y_1^*\Rightarrow\Lambda+\pi)$$

This branching ratio can be investigated by studying the K^-p interactions in which a Σ and two pions are produced. At present, the charged Σ events have been

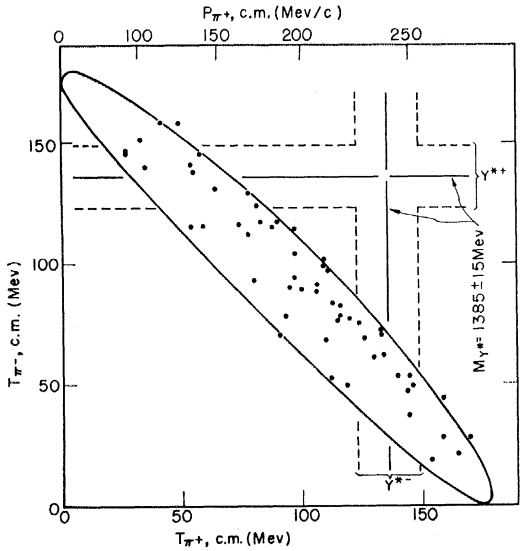

FIG. 15. Dalitz plot for the reaction $K^-+p\rightarrow\Sigma^0+\pi^+\pi^-$ at $P_{K^-}=760\pm 7.5$ Mev/c (55 events).

[17] R. H. Dalitz and D. H. Miller (to be published).
[18] R. K. Adair, Phys. Rev. **100**, 1540 (1955).

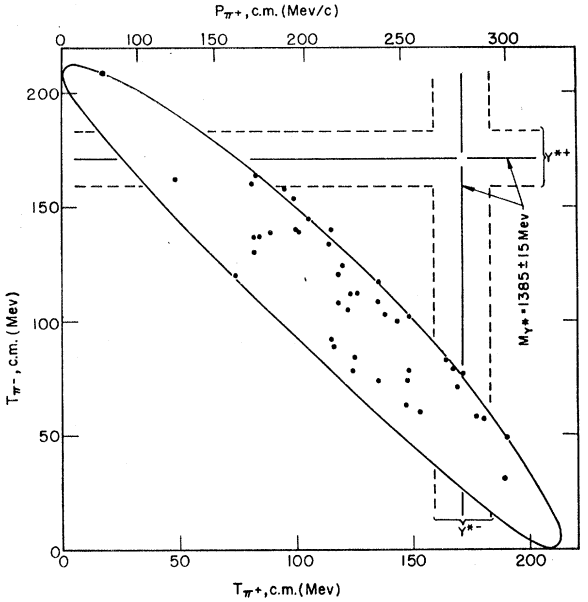

FIG. 16. Dalitz plot for the reaction $K^-+p \rightarrow \Sigma^0+\pi^++\pi^-$ at $P_{K^-}=850\pm10$ Mev/c (39 events).

analyzed only in the 1.15-Bev/c experiment.[19] The total cross sections for these events are shown in Table V.

Dalitz plots for uncharged Σ production at 760, 850, and 1150 Mev/c and charged Σ production at 1150 Mev/c are shown in Figs. 15–19. In order to derive values of R, two corrections were applied to the Σ^0 events. In these cases, only about $\frac{2}{3}$ of the events are observed because of neutral decays of the Λ, and some events are not plotted because they have an ambiguous Σ^0 or Λ interpretation (see Sec. III.A). The plotted events, therefore, were weighted appropriately to obtain the branching ratio R.

An upper limit for R($R_{\max}$ in Table VI) is found by assuming that all events in which the total energy of the $\Lambda-\pi$ and $\Sigma-\pi$ systems lies between 1355 and 1415 Mev are Y_1^* events. This treatment provides an unrealistic upper limit since there is obviously a large amount of background present. A more realistic value for R is obtained by subtracting a uniform phase-space background. At all incident momenta the results are consistent with $R=0$. This small value of the branching ratio for the strong decay of Y_1^* is in poor agreement with the predicted values quoted in the Introduction; however, it is more consistent with the global symmetry explanation of the resonance than with the $\bar{K}-N$ "bound-state" hypothesis. On the other hand, there seems to be little evidence for a resonance in the $\Sigma-\pi$ system at a total energy of about 1540 Mev, as predicted by the global-symmetry argument; but it must be noted that the distribution of events would be very insensitive to the presence of such a wide resonance.

[19] M. Alston, L. W. Alvarez, P. Eberhard, M. L. Good, W. Graziano, H. K. Ticho, and S. G. Wojcicki, Phys. Rev. Letters **6**, 300 (1961).

TABLE VI. Values of the branching ratio R for various incident K^- momenta.

K^- momentum (Mev/c)	R (%)	$R_{\max}$[c] (%)
760[a]	1±3	20
850[a]	−5±5	10
1150[b]	1±3	8

[a] $R=[Y^{*\pm} \rightarrow (\Sigma^0+\pi^\pm)]/[Y^{*\pm} \rightarrow (\Lambda+\pi^\pm)]$ at $P_{K^-}=760$ and 850 Mev/c.
[b] $R=\frac{1}{2}[Y^{*\pm} \rightarrow (\Sigma^0+\pi^\pm)+(\Sigma^\pm+\pi^0)]/[Y^{*\pm} \rightarrow (\Lambda+\pi^\pm)]$ at $P_{K^-}=1150$ Mev/c.
[c] $R_{\max}$ assumes that all the events with $1355<M_{Y^*}<1415$ are Y^*'s.

IV. EVIDENCE FOR Λ-π RESONANCE IN OTHER INTERACTIONS

A. Deuterium: The Reaction $K^-+d \rightarrow Y^*+p$

In a recent experiment at Berkeley in which K^- mesons were stopped in the deuterium-filled 15-in. bubble chamber,[3] the reactions

$$K^-+d \rightarrow \Lambda+\pi^-+p \quad (9)$$

$$\Sigma^0+\pi^-+p \quad (10)$$

$$\Sigma^-+\pi^0+p \quad (11)$$

were studied. The first two reactions can be separated by kinematics unless the recoil proton is too short to be measured. Figure 20 shows the Dalitz plot for 282 events of reaction (9). The proton energy spectrum for these events is plotted in Fig. 21.

The concentration of events in the region of the Dalitz plot where T_P is small and T_π is about 145 Mev can be easily explained. These are the results of K^- absorption on the neutron in the deuteron, in which the proton is a "spectator." An impulse model which assumes the K^- is absorbed from an atomic S orbital and which only includes the $\Lambda-p$ interaction in the final state is appropriate for this situation because the pion-nucleon system is produced in the weakly interacting $T=\frac{1}{2}$ state. Curve A in Fig. 21 shows the expected

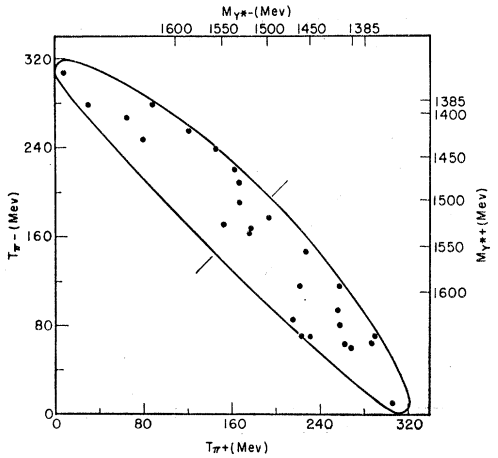

FIG. 17. Dalitz plot for the reaction $K^-+p \rightarrow \Sigma^0+\pi^++\pi^-$ at $P_{K^-}=1150\pm25$ Mev/c (27 events).

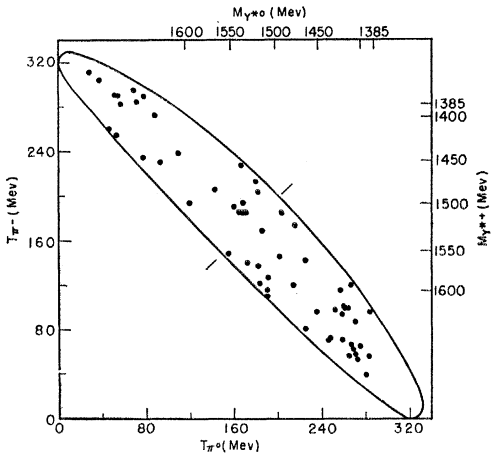

FIG. 18. Dalitz plot for the reaction $K^-+p \rightarrow \Sigma^+ + \pi^- + \pi^0$ at $P_{K^-}=1150\pm25$ Mev/c (57 events).

spectrum; it can be seen that this model fits qualitatively for $T_p<10$ Mev.

The events with pion energies near 92 Mev are explained by a two-step process in which the K^- interacts with one nucleon to form a Σ and π^- and the Σ then interacts with the other nucleon and is converted to a Λ. Since the conversion occurs mainly in the S-wave state of the $\Sigma-N$ system, lines of constant T_{π^-} in Fig. 20 are uniformly populated. The calculated curve B is shown in Fig. 21.

The theory accounts qualitatively for most of the proton and pion spectra, but there remains a group of events, with $T_p>10$ Mev and $T_{\pi^-}<100$ Mev, which are not explained. These anomalous events can be interpreted as the production of the $\Lambda\pi(Y_1^*)$ resonance. The curve drawn in Fig. 21 shows the effect of the resonance. The mass used is 1382 Mev and the half-width 20 Mev. It can be seen that a spectrum obtained by summing curves A, B, and C fits the data remarkably well. From this curve it is estimated that 93 events

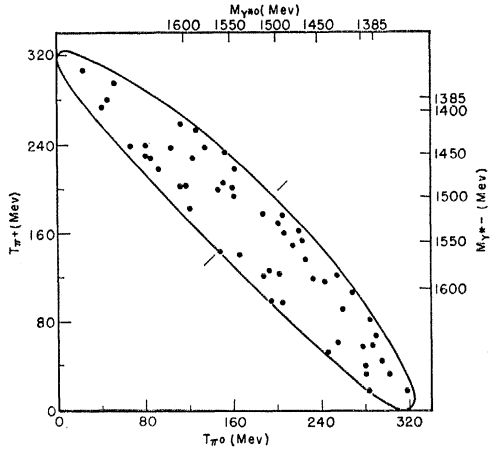

FIG. 19. Dalitz plot for the reaction $K^-+p \rightarrow \Sigma^- + \pi^+ + \pi^0$ at $P_{K^-}=1150\pm25$ Mev/c (55 events).

are associated with the resonant channel, 102 are internal conversions, and 87 are directly produced Λ's. Unfortunately, the data is insufficient to determine the spin and parity of the Y_1^*. It is estimated that 6% of all K^- absorptions proceed through the resonant $\Lambda\pi^-$ channel, whereas only 1.2% of stopped K's produce hyperons in nonmesic processes.

Reaction (11) was studied to obtain the branching ratio R. The events which are produced by the decay of Y_1^* appear in a region of the proton spectrum ($P_p\sim240$ Mev/c), which is unpopulated by the direct three-body production process. Twelve events were found with proton momentum >180 Mev/c giving an upper limit for R of 5%.

B. The Reaction $\bar{K}^0+p \rightarrow Y^*+\pi$

Adair discusses results on this reaction in some detail in one of the previous papers.[4] Again a $\Lambda\pi$ resonance is observed with $M_{Y_1^*}=1385$ Mev.

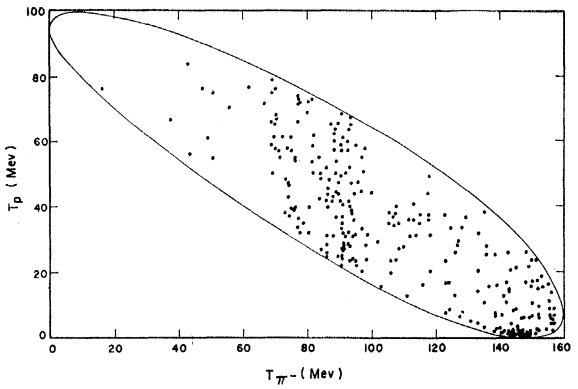

FIG. 20. Dalitz plot for the reaction $K^-+d \rightarrow \Lambda+\pi^-+p$ at $P_{K^-}=0$ Mev/c (282 events).

C. Helium: $K^-+\mathrm{He}^4 \rightarrow Y^*+\mathrm{He}^3$

Block *et al.* have studied 50 events of the type

$$K^-+\mathrm{He}^4 \rightarrow \Lambda+\pi^-+\mathrm{He}^3 \qquad (12)$$

produced when K^- mesons stopped in Duke University's helium bubble chamber.[5]

An impulse model predicts a phase-space peak in the He^3 momentum spectrum at 126 Mev/c, but the experimental peak is at 250 Mev/c. The observed spectrum can be explained by the production of Y_1^* with a mass of 1385 Mev and $\Gamma/2$ of 18 Mev. The decay angular distribution of the 30 events which have a He^3 momentum greater than 200 Mev/c and which are assumed to be due to Y_1^* production is isotropic. If the K^- is captured from an S orbital and a simple two-body ($Y_1^*+\mathrm{He}^3$) final-state model is used, then the decay distribution should be isotropic for a $J=\frac{1}{2}$ Y_1^* and of the form $1+3\cos^2\theta_{AY^*}$ for a Y_1^* of spin $\frac{3}{2}$. The

result therefore suggests that the spin of the Y_1^* is $\frac{1}{2}$. However, interference effects in the three-body final state may affect this conclusion. If the $K\Lambda$ parity is odd, then a $J=\frac{1}{2}$ Y_1^* is produced in an s state relative to the He^3 and subsequently decays via $S_{\frac{1}{2}}$ mode.

D. Propane: $K^-+p \rightarrow Y^*+\pi$ or $K^-+n \rightarrow Y^*+\pi$

Preliminary data obtained by the Powell group[6] using the Berkeley 30-in. propane bubble chamber show evidence, on a total of 60 analyzed events, for both Y^{*+}, Y^{*-}, and Y^{*0} production in the foregoing reactions.

V. CONCLUSIONS

The existence of the $\Lambda\pi$ resonance, its mass value of 1385±5 Mev and half-width of 25±5 Mev appear to be the only noncontroversial results now available. Other properties, such as spin, parity, excitation function, and decay branching ratio, are inconclusively determined at present. This unsatisfactory situation is mainly due to interference phenomena in the final state which complicate the interpretation of the data. These effects make it necessary to obtain more data; in particular, for the K^-p reactions, at incident momenta greater than 1000 Mev/c, where the interference effects should be of less importance.

This lack of a conclusive interpretation of the experimental data leaves the theoretical explanation of the resonance an open question.

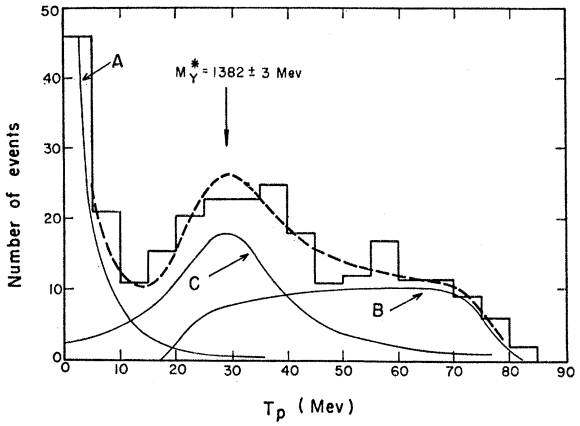

FIG. 21. Proton kinetic-energy spectrum for the reaction $K^-+d \rightarrow \Lambda+\pi^-+p$ at $P_{K^-}=0$ Mev/c.

ACKNOWLEDGMENTS

The authors are indebted to the many experimenters who furnished their data and allowed them to be included here. In particular, we would like to thank R. H. Dalitz, D. H. Miller, and A. H. Rosenfeld for their comments and advice.

DISCUSSION

R. H. Dalitz, *University of Chicago, Chicago, Illinois:* In view of the clear-cut evidence of the final state hyperon resonance which we have heard this afternoon, I would just like to make a few remarks concerning the possible interpretations of such a resonance. There are essentially two resonance mechanisms one can consider: firstly, as a property of the pion-hyperon system, that is, a resonance which would still remain even if the coupling to the K-meson system vanished; and secondly, that the resonance essentially reflects the property of the $\bar{K}$-meson nucleon interaction, and that this resonance in a certain sense corresponds to a bound state of the $\bar{K}$-nucleon system which then can decay into the pion-hyperon channels. There are several points in the data which bear on this, as the preceding speakers have mentioned. One is the width of the resonance. A resonance in a bound $\bar{K}$-nucleon system is possible only with zero energy scattering amplitudes in the $\bar{K}$-nucleon system which have a negative real part (with the sign convention that $k\cot\delta=1/A$). This confines the possibilities to two: the experimental data is such that the low energy scattering lengths may be characterized as $(a-)$ and $(b-)$ sets, where the property of the $(a-)$ set that it has a large $I=1$ real part for the scattering amplitude, while the imaginary part to the $(a-)$ scattering amplitude at zero energy is rather small. This is then the favored configuration if one interprets this resonance as a bound state of the $\bar{K}$-nucleon system. It is the property of this scattering data that the absorption in the $I=1$ channel is rather weak in the $I=1$ state. If I remember correctly, the parameters are 1.1±0.2 f for the real part of A_1, the imaginary part being 0.2 f. The $I=0$ amplitude in the same set of solutions gives approximately 1.7 f for the imaginary part of the scattering length, almost a factor of 10 larger. This is just to indicate the relative weakness of the absorption in the $\bar{K}-N$ $I=1$ channel. In interpreting this resonance as a bound $\bar{K}$-nucleon system, one of the main factors in giving a narrow width is the weakness of the absorption in that particular channel. To interpret the location of the resonance, the discussion which Tuan and I have given for the $\bar{K}$-nucleon system is inadequate because the resonance appears at an energy of −50 Mev, where the assumption of zero range theory is certainly not going to be adequate. This has been modified by Ross and Shaw, who have included an effective range in the amplitudes; with an effective range of about 0.5 f, which is a reasonable amount, the resonance is at roughly the right position. The difficulties of this interpretation are, first of all, that the experimental evidence which we have on low energy $\bar{K}$-proton scattering favors constructive interference with Coulomb scattering rather than the destructive interference predicted for the $(a-)$ set. Similarly the evidence on K-nucleus scattering indicates an attractive optical model potential, which appears contrary to this type of solution.

The second difficulty is the ratio of the Σ and Λ is unity, within a factor of 2. The simplest view is that the change in this branching ratio as one goes to the resonance state would mainly reflect changes in the centrifugal barriers for the outgoing $\pi\Sigma$ and $\pi\Lambda$ systems with decreasing available energy, as well as the reduction of phase space. If these are S-wave emissions, then it is somewhat hard to understand ratios which are as low as 10 or 5%, which is the limit quoted by the last speaker, unless one assumes that the Σ particle has, perhaps, negative parity, or opposite parity, relative to that of the Λ, so that a p-wave centrifugal barrier is effective in the Σ channel. I take it that the evidence which has been given by the last speaker is rather suggestive that $J=\frac{1}{2}$ with S waves is appropriate for the $\Lambda\pi$ system. The smallness of this ratio would require for this kind of interpretation that one

should certainly have p waves at least in the Σ decay channel. This is to be contrasted with the opposing picture which corresponds to global symmetry and which has been discussed in some detail by Amati, Stanghellini, and Vitale. This gives the correct location of the resonance and accounts for the branching ratio in a very natural way, but their interpretation does require that $J=\frac{3}{2}$ and I think there is no evidence of any angular distributions shown in any of the data we have seen today for the Y^* decay; one would certainly expect that, if $J=\frac{3}{2}$, an angular correlation should appear in one or the other of these processes

R. K. Adair, *Brookhaven National Laboratory, Upton, New York:* I would like to comment about our width, which has just been reported. It seems to be appreciably smaller than the width found in the work of Alston and others, but if one accepts it to be of the order of 20 Mev, one can compare this with the expected width from a relation similar to a sum rule in nuclear physics. One might expect a natural width for an elementary system to be related to a time equal to some radius, like a π Compton wavelength, divided by the speed of light. Such a width comes out to be 200 Mev which might be considered to be a natural width. A width of the order of 20 or 30 Mev, as we have just seen discussed here, would correspond to a very weak coupling to the $\Lambda\pi$ system and even weaker coupling in the $\Sigma\pi$ system. If we are going to use up this natural width in a sum rule with reasonably elementary operations, we might expect that the K^+-nucleon system would account for much of this, and this configuration might be described as a K-nucleon resonance.

Shaw, *University of California, La Jolla, California:* I would like to point out a possible way to explain this difference in the widths. Consider the Y^{*-}. In the Alston experiment the π^+ is clearly separated in energy from the energy of this resonance. But now at the lower energies connected with the experiment we have just heard reported, the other π is closer to the resonant energy so it can undergo a final state scattering with the Λ. Interference of these two effects, the decay of the Y^* and a final state scattering of the other π and the Λ, may cause some destructive interference and decrease the width. It is easier to interpret these experiments at the higher energies, when one π is clearly distinguishable in energy from the 1385-Mev resonance. Other interference effects, such as between the resonant production and the direct production of the three particle final state, may be important and should be looked at.

Weisskopf, *Massachusetts Institute of Technology, Cambridge, Massachusetts:* I would like to ask this simple question of the people who understand it: Why is it that one does not see the pion-pion resonance in these plots?

Selove, *University of Pennsylvania, Philadelphia, Pennsylvania:* In some work of Salant and company at Brookhaven, they saw what I think is the outstanding evidence for the pion-pion resonance. In a final state of proton-π^- and π^0, the $\pi^-\pi^0$ resonance shows up fairly strongly. In the final state where the charges are different, i.e., neutron $\pi^-\pi^+$, the π-π resonance is not seen. One obvious explanation is that the neutron π^- system is a pure $T=\frac{3}{2}$; the very strong $\frac{3}{2}$–$\frac{3}{2}$ resonance may just obscure the π-π resonance. It may be here that if one has a very strong π-Λ resonance, it just obscures the π-π resonance, if there really is a π-π resonance.

REVIEWS OF MODERN PHYSICS VOLUME 33, NUMBER 3 JULY, 1961

Some Speculations on the New Resonances

ABDUS SALAM

Imperial College, London, England

THIS has been an exciting Conference. We have heard of four resonances during two days—surely a record number for any conference. Table I summarizes the data presented. The first characteristic which strikes one most forcibly is the comparatively narrow width of these resonances. One way to bring this out (for example, for Y^* and K^*) is to assume S-wave couplings of the type $gY^*\Lambda\pi$ and $fK^*K\pi$ responsible for the (strong) decays of these particles. One finds $g^2/4\pi\sim 1/13$ and $f^2/4\pi\sim m_K^2/11$. Similarly, for an assumed direct decay of Λ^* to $N+\bar{K}$, one obtains $g^2/4\pi\sim\frac{1}{5}$. Thus, the interactions responsible for resonance widths are only "mildly" strong.

Dalitz has expressed this slightly differently. In the picture which he and Tuan are proposing, Y^* should be considered as a bound state of the $\bar{K}N$ system which would be completely stable if the mild pionic interactions were turned off. Y^*, then, is somewhat on the same footing, so far as the $\bar{K}N$ system is concerned, as the Λ and the Σ hyperons.

This line of thought inclines one more and more to the Goldhaber-Christy type of model of elementary particles. In these models, K mesons and nucleons are elementary entities, while all other particles are compounds made from these. Now it may or may not be possible to compute with present techniques the mass of a Λ hyperon or a π meson in such a model, but if we are slightly less ambitious and allow Λ's and π's also to be elementary, it is a remarkable fact that the Σ hyperon (considered as a bound state of $\pi\Lambda$ system) and the Y^* particle (considered as a bound state of $\bar{K}N$ system) possess nearly the same binding energy;

$$[m_\Sigma-(m_\Lambda+m_\pi)\approx m_{Y^*}-(m_K+m_N)\approx 50\text{–}60\ \text{Mev}].$$

Furthermore, this rather "mild" binding may even be amenable for calculations with even a rude potential model.

On pursuing this further, the experimental results presented at the Conference tend to indicate odd $(Y^*\Lambda)$ parity. On assuming the same $(K\pi)$ parity (same $K\Lambda$ and $\pi\Lambda$ parities, to be more precise), one may be tempted to infer from the near equality of